

# A Heterogeneous Schelling Model for Wealth Disparity and its Effect on Segregation

Zhanzhan Zhao\*

zhanzhanzhao@gatech.edu  
Georgia Institute of Technology  
School of Computer Science  
USA

Dana Randall\*

randall@cc.gatech.edu  
Georgia Institute of Technology  
School of Computer Science  
USA

## ABSTRACT

The Schelling model of segregation was introduced in economics to show how micro-motives can influence macro-behavior. Agents on a lattice have two colors and try to move to a different location if the number of their neighbors with a different color exceeds some threshold. Simulations reveal that even such mild local color preferences, or homophily, are sufficient to cause segregation. In this work, we propose a stochastic generalization of the Schelling model, based on both race and wealth, to understand how carefully architected placement of incentives, such as urban infrastructure, might affect segregation. In our model, each agent is assigned one of two colors along with a label, rich or poor. Further, we designate certain vertices on the lattice as “urban sites,” providing civic infrastructure that most benefits the poorer population, thus incentivizing the occupation of such vertices by poor agents of either color. We look at the stationary distribution of a Markov process reflecting these preferences to understand the long-term effects.

We prove that when incentives are large enough, we will have “urbanization of poverty,” an observed effect whereby poor people tend to congregate on urban sites. Moreover, even when homophily preferences are very small, if the incentives are large and there is income inequality in the two-color classes, we can get racial segregation on urban sites but integration on non-urban sites. In contrast, we find an overall mitigation of segregation when the urban sites are distributed throughout the lattice and the incentives for urban sites exceed the homophily biases. We prove that in this case, no matter how strong homophily preferences are, it will be exponentially unlikely that a configuration chosen from stationarity will have large, homogeneous clusters of agents of either color, suggesting we will have racial integration with high probability.

## CCS CONCEPTS

• **Mathematics of computing** → **Markov processes**; • **Theory of computation** → **Random walks and Markov chains**; • **Applied**

\*Corresponding authors. This work was supported by Georgia Tech ARC-TRIAD Fellowship, NSF Award CCF-2106687, CCF-1733812, and ARO MURI Award W911NF-19-1-0233.



This work is licensed under a Creative Commons Attribution International 4.0 License.

EAAMO '22, October 6–9, 2022, Arlington, VA, USA  
© 2022 Copyright held by the owner/author(s).  
ACM ISBN 978-1-4503-9477-2/22/10.  
<https://doi.org/10.1145/3551624.3555293>

**computing** → **Sociology**; • **Social and professional topics** → **Race and ethnicity**; **Geographic characteristics**.

## KEYWORDS

Schelling segregation model, wealth disparity, stochastic processes, stationary distribution, Peierls arguments

### ACM Reference Format:

Zhanzhan Zhao and Dana Randall. 2022. A Heterogeneous Schelling Model for Wealth Disparity and its Effect on Segregation. In *Equity and Access in Algorithms, Mechanisms, and Optimization (EAAMO '22)*, October 6–9, 2022, Arlington, VA, USA. ACM, New York, NY, USA, 10 pages. <https://doi.org/10.1145/3551624.3555293>

## 1 INTRODUCTION

Over fifty years ago, economist Thomas Schelling studied segregation by modeling residents as colored particles on a chessboard. Each particle is considered *happy* if its color agrees with more than a fixed fraction of its neighbors and *unhappy* particles try to move to new locations with more favorable neighborhoods [14]. Simulations reveal even a mild preference for neighbors of one’s own color is sufficient to cause segregation on a macroscopic scale [28]. Extensive work has been done by economists and sociologists to expand Schelling’s model using statistical analysis, simulation tools, and enhanced models [2, 16, 18, 32]. This work primarily focuses on how the dynamics determine the limiting distribution and try to connect the model to the real world population dynamics [7–9, 17, 25, 29, 33]. Recent work also seeks to understand the dual segregation of ethnicity and wealth with empirical studies [11, 24, 27].

Additional heuristical and rigorous studies on the implications of Schelling-like dynamics have been undertaken in the theoretical computer science and statistical physics communities, where the concept of micro-motives affecting macro-behavior such as phase transitions is well-understood. For instance, Brandt et al. [4, 12] rigorously determined the precise limiting distributions for the Schelling model in one dimension. Additional rigorous analysis was provided for a modified Schelling model with simplified neighborhood interactions [1, 26, 31] or with generalized local interactions [3, 30]. Bhakta et al. [3] introduced a randomized variant and proved that slight biases maintain well-integrated populations, whereas stronger biases lead to segregation. Unlike Schelling’s model where each person’s happiness has a deterministic threshold regarding one’s tolerance for differently colored neighbors, the model in [3] allows all particles to move stochastically and they are increasingly inclined to move when they have more neighbors of the opposite color. Improved bounds on the amount of bias that leads to integration and segregation were given by Cannon et al.

[5] for specific geometric incentive functions where the model can be mapped onto problems of heterogeneous particle separation in the programmable matter.

Most variants of the Schelling model assume that agents of each race are homogeneous and have identical incentives influencing where they prefer to live purely based on *homophily*, the desire for each particle to have neighbors that are similar to oneself, regardless of socio-economic status and location. However, such simple models cannot explain two widely observed phenomena: *centralization*, whereby one racial group clusters near the city center, and *urbanization of poverty*, whereby city centers and other areas dense with public amenities and infrastructure disproportionately attract the poorer populations. Centralization is widely-used to measuring racial segregation in metropolitan areas [15, 22]. Urban economists show that urbanization of poverty results from better access to public transportation in central cities and other resources [13]. Such evidence shows us that socio-economic considerations such as the spatial distributions of urban infrastructure are significant factors influencing racial segregation but these are not captured by any of the theoretical models. This motivated our work which simultaneously considers both homophily and each individuals' incentives according to their wealth level and their access to public amenities. With our proposed new model, we are able to rigorously explore the impact of wealth disparity on racial segregation, as well as civic interventions to potentially help mitigate segregation.

## 1.1 The heterogeneous Schelling model

To better understand these socioeconomic distinctions and the effects of economic disparity within a city, we introduce a new *heterogeneous Schelling model* where individuals are each assigned a color and designated *rich* or *poor*. We also distinguish some vertices on the underlying lattice to be *urban sites* if they provide useful infrastructure (or resources) that is most beneficial to poor citizens. The urban sites might be grouped centrally, for instance representing a metropolitan city center, or distributed evenly throughout large parts of the city, representing a vast public transportation network or other distributed amenities (see Fig 1). While all individuals have uniform homophily preferences, as in the standard Schelling model, we add additional incentives that favor configurations with more poor people residing on urban sites, capturing the presumption that urban sites provide sufficient benefits to poor individuals to incentivize their relaxing their racial biases. We are interested in understanding when urban infrastructure can help mitigate racial biases and lessen segregation for various placements of urban sites for such a model.

Specifically, we represented the city by a finite torus on the triangular lattice, with each site accommodating exactly one person. Each person (or agent) is blue or red, representing race, and *rich* or *poor*, representing wealth. The vertices  $\mathcal{U} \subseteq \mathcal{V}$  are the *urban sites*. Each pair of neighbors has homophily (or racial) bias  $\lambda$ , representing how much they each prefer neighbors of their own color. Setting  $\lambda > 1$  is the "ferromagnetic" setting corresponding to agents preferring same-colored neighbors. Further, poor agents have an affinity for urban sites with a wealth bias parameter  $\gamma$ ; setting  $\gamma > 1$  biases poor agents to prefer residing on urban sites. When  $\gamma = 1$ , we recover the pure standard homophily model where wealth of individuals is

not considered. Let  $\Omega = (\{\text{red, blue}\} \times \{\text{rich, poor}\})^{|\mathcal{V}|}$  be the state space. The stationary probability of any configuration  $\sigma \in \Omega$  is given by

$$\pi(\sigma) = \lambda^{-h(\sigma)} \gamma^{p(\sigma)} / Z,$$

where  $h(\sigma)$  is the number of racially heterogeneous edges (whose endpoints do not share the same color),  $p(\sigma)$  is the number of poor agents on urban sites, and

$$Z = \sum_{\sigma \in \Omega} \lambda^{-h(\sigma)} \gamma^{p(\sigma)}$$

is the normalizing constant.

A randomized algorithm  $\mathcal{M}$  for sampling from  $\pi$  can be described as follows. At each time step, two random agents are selected, and they swap locations with the appropriate Metropolis probabilities so as to converge to  $\pi$ . In particular, they are more likely to swap if they are each in less homogeneous neighborhoods, as previously studied in [3, 5], with an additional bias toward keeping poor agents on urban sites, so happier individuals are less likely to move. We note that when there are no urban sites (or all vertices are urban sites), then the wealth of individuals becomes irrelevant and we recover the racial segregation model studied in [5], where the dichotomy of the phase change between integration and segregation has been proved. Here we are interested in the effects in heterogeneous cases where both urban and non-urban sites are present. We also require the size of the urban sites to be of a constant fraction of the total sites. For topology, we study the impact of the centralized or distributed placement of the urban sites on segregation.

## 1.2 Effects on wealth and racial segregation

First, we show that our model yields *urbanization of poverty* when the wealth bias  $\gamma$  is sufficiently large, with all but an arbitrarily small fraction of urban sites being occupied by poor agents. Conversely, we show that for any racial bias  $\lambda > 1$ , if the wealth bias  $\gamma > 1$  is small enough, then it is exponentially unlikely that poor agents will be disproportionately concentrated on urban sites.

Moreover, when the urban sites are centralized and both racial bias  $\lambda$  and wealth bias  $\gamma$  are large enough, *urbanization of poverty* and *racial segregation* will occur simultaneously. However, when there is significant inequality in the distribution of wealth and many more poor people come from one race, then even when the racial bias  $\lambda$  is small, as long as the wealth bias  $\gamma$  is large, we will have *racial segregation on urban sites* and *racial integration on the non-urban sites*. This suggests that the urbanization of poverty can enhance racial segregation when the infrastructure is centralized, such as with a dense city center with civic services and perhaps subsidized housing, providing a primary location that incentivizes occupation by poor people.

We show there will be a dramatically different outcome when the urban sites are well-distributed throughout the city, such as with public transportation stops that service the entire city. First, we prove under income inequality, where one race has a higher proportion of poor people, no matter how large racial bias  $\lambda$  is, as long as the wealth bias  $\gamma$  exceeds racial bias  $\lambda$  sufficiently, both the urban and non-urban sites will be integrated with high probability. That is, the probability of large spatial clusters with predominantly one race forming anywhere is exponentially small. This suggests that distributing urban infrastructure equitably throughout the

city will have a better effect on mitigating segregation when the incentives are large enough compared to the inherent racial biases.

Our proofs build on *Peierls arguments* from statistical physics for the integration and separation of heterogenous particles in the context of programmable matter [5]. The essential idea is to map the set of configurations not satisfying a target property to a set of configurations that have exponentially larger probability at stationarity, so that the inverse maps do not require significant information, thus proving that configurations outside of the target set must have small probability by evaluating “energy/entropy” balancing the probabilities and the number of preimages. However, the introduction of urban sites and wealth bias greatly complicates the proofs as we have to keep the same number of people for each pair of wealth level and race before and after the mapping  $v = f(\sigma)$ . In our setting, all four groups may deviate under the maps and it requires careful arguments to be able to restore the cardinalities of all the sets without losing too much information about the inverse map, which is significantly more challenging than earlier proofs that only considered race.

## 2 PRELIMINARIES

The dynamics we study can be viewed as a Markov chain that converges to a distribution reflecting the overall effects of individual biases. We briefly review properties of Markov chains and summarize techniques used to analyze their stationary distributions.

### 2.1 Markov chains

A Markov chain is a memoryless random process on a state space  $\Omega$ , which is finite and discrete in our setting. We focus on discrete time Markov chains, where one transition occurs per time step. The transition matrix  $M$  on  $\Omega \times \Omega \rightarrow [0, 1]$  is defined so that  $M(x, y)$  is the probability of transiting from state  $x$  to state  $y$  in one step, for any pair  $x, y \in \Omega$ . The  $t$ -step transition probability  $M^t(x, y)$  is the probability of moving from  $x$  to  $y$  in exactly  $t$  steps.

A Markov chain is *irreducible* if for all  $x, y \in \Omega$ , there exists a  $t$  such that  $M^t(x, y) > 0$  and is *aperiodic* if for all  $x, y \in \Omega$ ,  $\text{g.c.d.}\{t : M^t(x, y) > 0\} = 1$ , where g.c.d. stands for the greatest common divisor. A Markov chain is *ergodic* if it is *irreducible* and *aperiodic* (see, e.g., [20]).

A *stationary distribution* of a Markov chain is a probability distribution  $\pi$  over the state space  $\Omega$  such that  $\pi P = \pi$ . Any finite, ergodic Markov chain converges to a unique stationary distribution given by  $\pi(y) = \lim_{t \rightarrow \infty} P^t(x, y)$  for any  $x, y \in \Omega$ ; moreover, for such chains the stationary distribution  $\pi(y)$  is independent of starting state  $x$ . To verify  $\pi$  is the unique stationary distribution of a finite ergodic Markov chain, it suffices to check the *detailed balance condition*, i.e.,  $\pi'(x)M(x, y) = \pi'(y)M(y, x)$  and  $\sum_{x \in \Omega} \pi'(x) = 1$  for all  $x, y \in \Omega$  (see [10]).

### 2.2 Peierls arguments

Peierls arguments are helpful in analyzing a chain’s limiting behavior by showing that the probability a sample drawn from the stationary distribution  $\pi$  of a Markov chain falls into some target set is exponentially small in  $n$ , indicating that  $\pi(\Omega_t) \leq \xi^n$  for some constant  $\xi \in (0, 1)$ . The Peierls argument is based on a map from configurations in the target set  $\Omega_t$  to configurations in the

configuration space  $\Omega$  such that the map has an exponential gain in probability. Thus the targeted configurations are exponentially unlikely in  $\Omega$ . Mathematically, the mapping  $v = f(\sigma)$  is defined from  $\sigma \in \Omega_t$  to  $v \in \Omega$ , which yields

$$\begin{aligned} \pi(\Omega_t) &= \sum_{\sigma \in \Omega_t} \pi(\sigma) \leq \sum_{v \in \Omega} \sum_{\sigma \in f^{-1}(v)} \pi(\sigma) \\ &= \sum_{v \in \Omega} \pi(v) \frac{\sum_{\sigma \in f^{-1}(v)} \pi(\sigma)}{\pi(v)}. \end{aligned} \quad (1)$$

In order to show  $\pi(\Omega_t) \leq \xi^n$ , the mapping needs to be carefully defined to get the upper bounds of the probability ratio  $\frac{\pi(\sigma)}{\pi(v)}$  and the number of the preimages  $|f^{-1}(v)|$  for any given  $v$ . A mapped configuration  $v$  with large probability ratio  $\frac{\pi(\sigma)}{\pi(v)}$  can also have many possible preimages, which necessitates carefully balancing  $\frac{\pi(\sigma)}{\pi(v)}$  and  $|f^{-1}(v)|$ , representing an *energy/entropy tradeoff*.

To facilitate the mapping operations  $f(\cdot)$  and the counting of  $|f^{-1}(v)|$ , certain *bridge systems* have been introduced in [5, 23] to efficiently encode some information about mapped configurations to facilitate inverting the map and help bound the number of preimages. Unlike [5, 23], here the configuration space is enlarged by the introduction of a wealth dimension, requiring extending the bridge system to encode multi-dimensional information representing race and wealth. Moreover, because the additional wealth term is reflected in the stationary distribution, more careful mapping rules are required to account for tradeoffs between  $\frac{\pi(\sigma)}{\pi(v)}$  and  $|f^{-1}(v)|$ , balancing the effects of both the wealth and homophily biases in the probability measure.

## 3 THE HETEROGENEOUS SCHELLING MODEL WITH INCENTIVES

In our proposed model, a city is represented by a finite toroidal region of the triangular lattice  $G_\Delta = (\mathcal{V}, \mathcal{E})$ , shown in Figure 1a. Each vertex in  $\mathcal{V}$  represents a potential residence or *site*. Two adjacent vertices are *neighboring sites*, and each site has six nearest neighbors on  $G_\Delta$ . Some vertices  $\mathcal{U} \subseteq \mathcal{V}$  are designated *urban sites*. We denote the set of agents as  $\mathcal{A}$  and the poor agents as  $\mathcal{P} \subseteq \mathcal{A}$ . Figure 1a shows an example of centralized placement of urban sites, whereas Figure 1b shows the distributed placement, with urban sites depicted as yellow hexagons.

We assume each agent  $i$  is assigned a race  $r(i) \in \{\text{blue, red}\}$  and wealth  $w(i) \in \{\text{rich, poor}\}$ . Each site in  $\mathcal{V}$  can accommodate at most one agent. For simplicity of analysis, we assume that  $n$  agents fully occupy all the sites on  $G_\Delta$ , where  $|\mathcal{V}| = n$ . The size of the urban sites is assumed to be of a constant fraction of all the sites, i.e.,  $|\mathcal{U}| = c \cdot n$ , where  $c \in [0, 1]$ . As shown in Figure 1c, we represent the race of an agent by color and the wealth of an agent by the shade of each color; poor blue agents are referred to as *cyan*, poor red agents are *pink* and *blue* and *red* are reserved for the rich members of each color class.

Among the  $n$  agents,  $\mathcal{P}$  is the subset that are poor; the fraction that are poor is denoted by  $p$ , so  $|\mathcal{P}| = p \cdot n$ . Similarly, the fraction of red agents  $\mathcal{R}$  is  $r$ , with  $|\mathcal{R}| = r \cdot n$ . Among the red agents, we further denote the fraction of poor red agents  $\mathcal{R}_p$  as  $r_p$ , and the fraction of rich red agents  $\mathcal{R}_r$  as  $r_r$ , so that  $|\mathcal{R}_p| = r_p n$ , and  $|\mathcal{R}_r| = r_r n$ . Similarly,

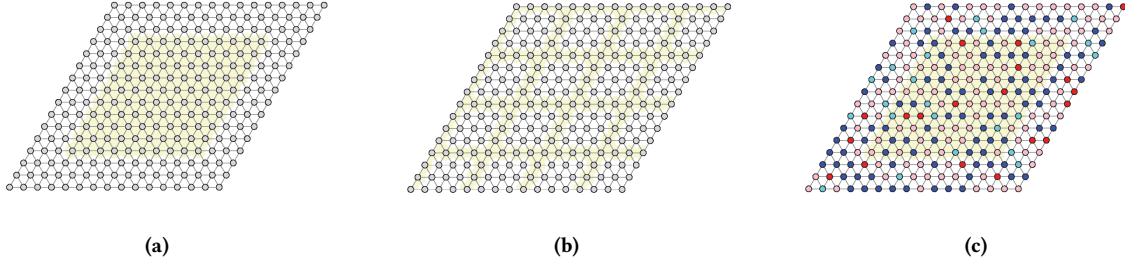


**Figure 1: A city lattice region  $G_\Delta$  (a) with centralized urban sites (shaded in yellow), (b) with distributed urban sites, and (c) centralized and fully occupied by the four types of agents.**

we define the fraction of the blue  $\mathcal{B}$  as  $b$ , the fraction of poor blue  $\mathcal{B}_p$  as  $b_p$ , and the fraction of rich blue as  $\mathcal{B}_r$  as  $b_r$ .

A *configuration* (or a *state*)  $\sigma$  is an assignment of the four types (race and wealth) to each of the vertices of  $G_\Delta$ . The *state space* (or configuration space)  $\Omega = (\{\text{red, blue}\} \times \{\text{rich, poor}\})^{|\mathcal{V}|}$  is the set of all possible configurations.

For a configuration  $\sigma$ , we denote  $\ell_\sigma(i) \in \mathcal{V}$  as the site where agent  $i$  resides. Agents living at adjacent sites are *neighbors* and each agent has six neighbors. Each agent  $i$  is assigned a race  $r(i)$ , wealth  $w(i)$ , and occupies a site  $\ell_\sigma(i)$ , which it can recognize as an urban site or not. We define an indicator function that takes agent  $i$  as input and outputs true when  $i$  is poor and currently on the urban sites as the following:

$$u_\sigma(i) \triangleq \begin{cases} 1, & \text{if } i \in \mathcal{P}, \ell_\sigma(i) \in \mathcal{U} \\ 0, & \text{otherwise} \end{cases}$$

For a configuration  $\sigma$ , the number of agents that are both poor and on the urban sites is defined to be  $p(\sigma) \triangleq \sum_{i \in \mathcal{A}} u_\sigma(i)$ .

For each agent  $i$ , let  $N_\sigma(i)$  be the number of neighbors of  $i$  that share its color. An edge in a configuration  $\sigma$  with vertices occupied by agents  $i$  and  $j$  is *racially homogeneous* if their colors agree (i.e.,  $r(i) = r(j)$ ) and *racially heterogeneous* otherwise. We define the total number of racially heterogeneous edges of a configuration  $\sigma$  as  $h(\sigma)$ , and the total number of racially homogeneous edges as  $e(\sigma)$ .

The Markov chain  $\mathcal{M}$  is defined so that it will converge to  $\pi(\sigma) = \lambda^{-h(\sigma)} \gamma^{p(\sigma)} / Z$ , which generalizes the Schelling probabilities to reflect the additional contribution of urban sites. Each agent  $i$  is able to swap locations with any agent  $j \in \mathcal{A}$ ,  $j \neq i$  in the city  $G_\Delta$ , which we denote it a *swap move*  $s_{ij}$ . Beginning with any configuration  $\sigma_0 \in \Omega$ , at each time step, the algorithm randomly picks two agents  $i$  and  $j$  at sites  $\ell_\sigma(i) \in \mathcal{V}$  and  $\ell_\sigma(j) \in \mathcal{V}$  and tries to swap their positions with the appropriate Metropolis probabilities (so agents are more likely to move if the move increases its number of racially homogeneous neighbors, but with a dampening factor  $\frac{1}{\gamma} < 1$  if the agent is poor and currently at the urban site. Mathematically,

$$P(\sigma : i \rightarrow j) = \frac{\lambda^{-N_\sigma(i)}}{\gamma^{u_\sigma(i)}},$$

where  $\lambda > 1$ , and  $\gamma > 1$ . The probability of agents  $i$  and agent  $j$  swapping positions satisfies

$$P(\sigma : s_{ij}) = \frac{1}{n^2} \lambda^{-N_\sigma(i) - N_\sigma(j)} \gamma^{-\sum_{k \in \{i, j\}} u_\sigma(k)}. \quad (2)$$

---

**Algorithm 1** Markov Chain  $\mathcal{M}$ .

---

**Beginning at any configuration  $\sigma_0$  with  $n$  agents, repeat:**

Choose two agents  $i$  and  $j$  uniformly at random in the current configuration  $\sigma$ .

Choose  $q \in (0, 1)$  uniformly at random.

**if**  $q < \lambda^{-N_\sigma(i) - N_\sigma(j)} \gamma^{-\sum_{k \in \{i, j\}} u_\sigma(k)}$  **then**  
agents  $i$  and  $j$  swap positions.

**else**

agents  $i$  and  $j$  keep their current locations.

**end if**

---

It is easy to see that the Markov chain  $\mathcal{M}$  is ergodic on the state space  $\Omega$ , since swap moves of  $\mathcal{M}$  suffice to transform any configuration to any other configuration (irreducible) and there is a non-zero self-loop probability for  $\lambda > 1$  and  $\gamma > 1$  (aperiodic). Using detailed balance it is easy to confirm that the Markov chain converges to

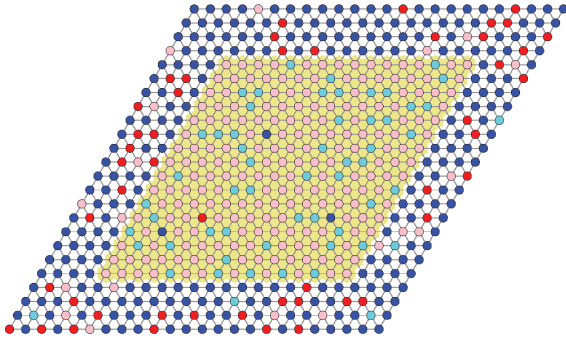
$$\pi(\sigma) = \lambda^{-h(\sigma)} \gamma^{p(\sigma)} / Z, \quad (3)$$

with  $h(\sigma)$  the number of racially heterogeneous edges in  $\sigma$ ,  $p(\sigma)$  represent the number of poor people on the urban sites in  $\sigma$ , and  $Z = \sum_{\sigma \in \Omega} \lambda^{-h(\sigma)} \gamma^{p(\sigma)}$  the partition function that normalizes the probability distribution. See Section 1.1 of Supplementary Information (SI) for proof details.

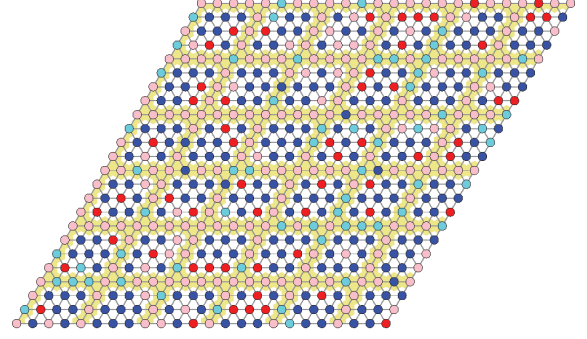
## 4 URBANIZATION OF POVERTY

We begin by confirming the *urbanization of poverty*, whereby a  $1 - \epsilon$  fraction of the urban sites are occupied by poor agents, for any constant  $\epsilon > 0$ . We prove in Theorem 2 that under *centralized placement*, for any  $\lambda$  and  $\epsilon$ , and  $\gamma$  sufficiently large, urbanization of poverty will occur at stationarity with high probability. See Figure 2a for simulations. Further, in Corollary 3 we prove that when urban sites are distributed throughout the lattice, for any  $\epsilon$  and  $\lambda$  with  $\gamma > \lambda$ , we again will have urbanization of poverty (simulations in Figure 2b). Finally, we prove that for centralized urban sites, if  $\gamma > 1$  and  $\epsilon > 0$  are sufficiently small, then for any  $\lambda > 1$ , we are very unlikely to have urbanization of poverty, i.e., more than a  $1 - \epsilon$  fraction of urban sites will be occupied by rich agents.

**Definition 1.** For any  $\epsilon \in (0, \frac{1}{2})$ , a city is said to have  $\epsilon$ -**urbanization of poverty** if the number of poor agents on the urban sites is at least  $\min\{c, p\}n - \epsilon n$ .



(a) mixed urbanization and racial integration outside the centralized urban sites, with  $\gamma = 200, \lambda = 1.01$ .



(b) urbanization of poverty and integration with distributed urban sites with  $\gamma = 200, \lambda = 1.01$ .

**Figure 2: Simulations of  $\mathcal{M}$  after five million iterations with 40% poor red(pink), 10% rich red (red), 40% rich blue (blue), and 10% poor blue (cyan) and a 46% fraction of the urban sites.**

The parameter  $\epsilon$  captures the tolerance for allowing rich agents on urban sites: smaller  $\epsilon$  indicates a higher density of poor agents on urban sites, whereas larger  $\epsilon$  allows a larger fraction to be occupied by rich agents. The term  $\min\{c, p\}n$  is the maximum possible occupancy of poor agents on urban sites for given populations. Hence,  $\epsilon$ -urbanization of poverty requires that the maximum number of poor agents occupy urban sites, leaving at most an  $\epsilon$  fraction to be occupied by rich agents.

First, we show in Theorem 2 and Corollary 3 that for either centralized urban sites or distributed urban sites, if  $\gamma$  is sufficiently large, then we are likely to observe urbanization of poverty at stationarity.

**Theorem 2 (Centralized Urbanization of Poverty).** *If  $\gamma > 16 \frac{3(3\epsilon+2)}{2\epsilon^2}$  and  $\lambda > 1$ , with the centralized urban sites, when  $n$  is sufficiently large, then for  $\mathcal{M}$ , configurations drawn from distribution  $\pi$  have  $\epsilon$ -urbanization of poverty with probability at least  $1 - \xi_1^n$ , where  $0 < \xi_1 < 1$ .*

To prove this theorem, we first define  $\Omega_{\text{-urb}}$  to be the set of the configurations that do not have  $\epsilon$ -urbanization of poverty. It suffices to show  $\pi(\Omega_{\text{-urb}}) \leq \xi_1^n$ . We use Peierls argument using a mapping from non-urbanized configurations to urbanized configurations, along with appropriate *bridging*, to show that the image of the map has an exponentially higher probability than their preimages. With careful counting, this lets us conclude that non-urbanized configurations are exponentially less likely than urbanized ones, even though there are many more non-urbanized configurations and some of those configurations can have large probability weights in terms of  $\lambda^{-h(\sigma)}$ .

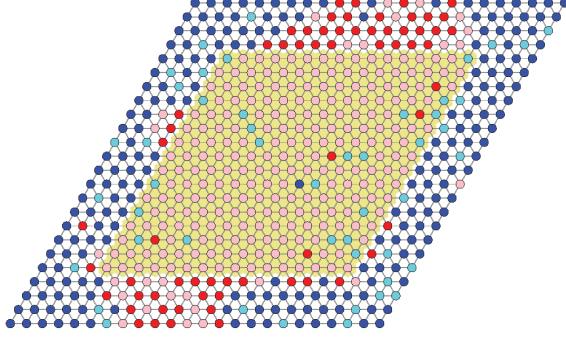
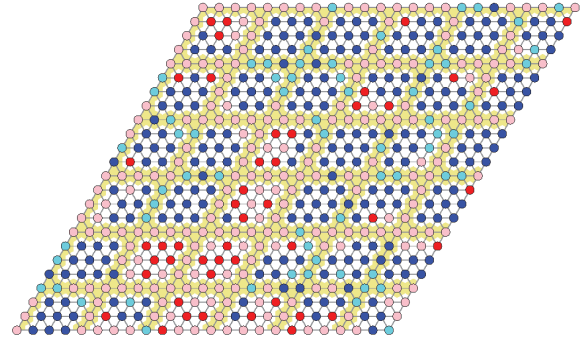
While similar to [5, 23], the addition of a wealth in the model requires significantly modifying the bridge systems to encode both race and wealth for each agent using a  $\delta$ -race\_wealth bridge system, as specified in Section 1.2 of SI. Here we have to carefully account for additional effects contributing the energy term because some configurations with large probability  $\gamma^{p(\sigma)-p(v)}$  can be mapped to configurations with small weight  $\lambda^{-(h(\sigma)-h(v))}$ . This necessitates

designing more careful mapping rules to balance  $\frac{\pi(\sigma)}{\pi(v)}$  and  $|f^{-1}(v)|$ ; see Section 1.3-1.5 of SI for details of the mapping.

**PROOF OF THEOREM 2.** For any  $\sigma \in \Omega_{\text{-urb}}$ , we first construct a  $\delta$ -race\_wealth bridge system (see Section 1.2 of SI for definition and Figure 2a of SI for illustration) and define the mapping  $f(\sigma) = (f_5 \circ f_4 \circ f_3 \circ f_2 \circ f_1)(\sigma)$ , where  $\psi = f_1(\sigma)$  is the richness inversion mapping (defined in Section 1.3 of SI and see Figure 2b in SI for illustration), and  $\tau = f_2(\psi)$  is the color inversion mapping (defined in Section 1.3 of SI and see Figure 2b in SI for illustration).  $\tau = (f_2 \circ f_1)(\sigma)$  eliminates the bridged racially heterogeneous edges and the bridged poor agents. For  $(f_5 \circ f_4 \circ f_3)(\tau)$  (defined in Section 1.4 of SI, we first assume the urban sites are centralized, under which we recover the same ratios of each color and richness as in  $\sigma$  in the centralized way defined in Section 1.5 of SI (also see Figure 3 in SI for illustrations). Then the upper bounds of  $h(v) - h(\sigma) \leq 3\alpha\sqrt{n} - z_c$  and  $p(\sigma) - p(v) \leq -\delta n$  and  $|f^{-1}(v)| \leq (z_c + 1)9^\alpha \sqrt{n} 4^{\frac{3\delta+1}{4\delta}} (z_c + 3n)$  can be obtained from Claim 15 and 16 in Section 2 of SI. The color contour length  $z_c$  is defined in the bridge system (Section 1.2 of SI), which is the sum of the length of the contours separating the red (or pink) from the blue (or cyan) in  $\sigma$  with a no more than  $\delta$ -fraction omission. Finally, substituting (3) and our other bounds into the Peierls argument yields

$$\begin{aligned} \pi(\Omega_{\text{-urb}}) &= \sum_{\sigma \in \Omega_{\text{-urb}}} \pi(\sigma) \leq \sum_{v \in \Omega} \sum_{\sigma \in f^{-1}(v)} \pi(\sigma) \\ &= \sum_{v \in \Omega} \pi(v) \frac{\sum_{\sigma \in f^{-1}(v)} \pi(\sigma)}{\pi(v)} \\ &\leq \sum_{v \in \Omega} \pi(v) \sum_{\sigma \in f^{-1}(v)} \lambda^{h(v)-h(\sigma)} \gamma^{p(\sigma)-p(v)} \\ &\leq \sum_{v \in \Omega} \pi(v) \sum_{z_c = \sqrt{r-n}}^{3n} a(n)(z_c + 1) \left( \frac{4^{\frac{3\delta+1}{4\delta}}}{\lambda} \right)^{z_c} \left( \frac{64^{\frac{3\delta+1}{4\delta}}}{\gamma^\delta} \right)^n, \end{aligned}$$

where  $a(n) \triangleq (3n + 1) \cdot 9^\alpha \sqrt{n} n^6$ ,  $z_c \leq 3n$  is because the color contour length is upper bounded by the sum of all edges of  $G_\Delta$ ,

(a) urbanized segregation with  $\gamma = 200, \lambda = 2$ .(b) mitigation of segregation via distributing the urban sites, with  $\gamma = 200, \lambda = 2$ .

**Figure 3: Simulations of  $\mathcal{M}$  after five million iterations with 40% poor red (pink), 10% rich red (red), 40% rich blue (blue), and 10% poor blue (cyan) and a 46% fraction of the urban sites.**

and  $z_c \geq \sqrt{r \cdot n}$  is due to the triangular lattice geometry, which is proved in Lemma 2.1 in [6].

If  $\lambda \geq 4^{\frac{3\delta+1}{4\delta}}$ , as long as  $\gamma^{\delta/3} > 4^{\frac{3\delta+1}{4\delta}}$ , the sum will be exponentially small for sufficiently large  $n$ . Or if  $1 \leq \lambda < 4^{\frac{3\delta+1}{4\delta}}$ , the sum further yields  $\pi(\Omega_{\text{-urb}}) \leq n^6 \cdot (3n+1) \cdot 9^{\alpha\sqrt{n}} \cdot 3n \cdot \left(\frac{16}{\lambda\gamma^{\delta/3}}\right)^{3n}$ . As long as  $\gamma^{\delta/3} > 16^{\frac{3\delta+1}{4\delta}} \geq 16^{\frac{3\delta+1}{4\delta}}/\lambda$ , the sum will still be exponentially small for sufficiently large  $n$ . Combining the two cases, we can see that as long as  $\gamma^{\delta/3} > 16^{\frac{3\delta+1}{4\delta}}$  and  $\lambda > 1$ ,  $\pi(\Omega_{\text{-urb}}) \leq \xi_1^n$ , for  $\xi_1 \in (0, 1)$ . Substituting  $\delta = \epsilon/2$  into  $\gamma^{\delta/3} > 16^{\frac{3\delta+1}{4\delta}}$  yields Theorem 2.  $\square$

In the above theorem, to realize the urbanization of poverty under the centralized urban sites placement, it suffices to have  $\lambda \cdot \gamma^{\delta/3} > 16^{\frac{3\delta+1}{4\delta}}$ , where the wealth bias and the racial bias both contribute to the urbanization of poverty. In contrast, when urban sites are distributed, we find competing effects between  $\gamma$  and  $\lambda$ , whereby urbanization of poverty is achieved when  $\gamma$  is strictly larger than  $\lambda$ . See detailed proofs in Section 3 of SI.

**Corollary 3 (Distributed Urbanization of Poverty).** *If  $\gamma > 4^{\frac{3(3\epsilon+2)}{2\epsilon^2}} \cdot \max\{\lambda^{6/\epsilon}, 4^{\frac{3(3\epsilon+2)}{2\epsilon^2}}\}$  and  $\lambda > 1$ , with the distributed urban sites, when  $n$  is sufficiently large, then for  $\mathcal{M}$ , configurations drawn from distribution  $\pi$  have  $\epsilon$ -urbanization of poverty with probability at least  $1 - \xi_1^n$ , where  $0 < \xi_1 < 1$ .*

On the other hand, when the incentives for the poor agents to occupy urban sites are small, urbanization of poverty will not occur. In particular, we prove in Theorem 4 that for any  $\lambda > 1$ , if  $\gamma > 1$  but is smaller than a threshold, it is exponentially unlikely we will observe urbanization of poverty at stationary under certain demographic parameter choices. See the proof details in Section 4 of SI.

**Theorem 4 (Dispersion of Poverty).** *Given centralized urban sites,  $p < c < p + \epsilon$ ,  $r_p < r_r - \delta$  and  $b_p < b_r - \delta$ , for any  $\lambda > 1$ , if*

$1 < \gamma < \left(\frac{r-\delta}{r_p}\right)^{\frac{r_p}{p}} \left(\frac{b-\delta}{b_p}\right)^{\frac{b_p}{p}} / 2$ , when  $n$  is sufficiently large, then for  $\mathcal{M}$ , configurations drawn from distribution  $\pi$  have  $\epsilon$ -urbanization of poverty with probability at most  $\xi_2^n$  for some constant  $0 < \xi_2 < 1$  and  $\delta = \frac{\epsilon}{2}$ .

## 5 URBANIZED RACIAL SEGREGATION

Next, we explore conditions that lead to *urbanized racial segregation*, where the large regions in the urban sites are occupied by poor agents of predominantly one race. We define  $(\beta, \delta)$ -**segregation** as follows.

**Definition 5.** *For  $\beta > 4\sqrt{r}$  and  $\delta \in (0, \frac{1}{2})$ , a city configuration  $\sigma$  is said to be  $(\beta, \delta)$ -**segregated** if there exists a subset of agents  $R$  such that:*

- *there are at most  $\beta\sqrt{n}$  racially heterogeneous edges of  $\sigma$  with exactly one endpoint in  $R$ ;*
- *the number of red agents in  $R$  is at least  $rn - \delta n$ .*

The parameter  $\delta$  is the tolerance for having agents of the other color within the red region  $R$ , with smaller  $\delta$  corresponding to a increased segregation. If one color class has fewer than  $\delta n$  agents, then the entire configuration space will be  $(\beta, \delta)$ -segregated, with  $R = \emptyset$ , or  $\bar{R} = \emptyset$ . We require that each color class has more than  $\delta n$  agents and, accordingly, we need  $\delta < 1/2$ . The parameter  $\beta$  controls how small the boundary is between the red region  $R$  and the rest of the configuration, and the minimal value  $4\sqrt{r}$  corresponds to the extremal case where the red region forms a homogeneous hexagonal cluster. We say that a configuration  $\sigma$  is **integrated** if the city is not  $(\beta, \delta)$ -segregated for any  $\beta$  and  $\delta$ .

**Definition 6.** *For  $\beta > 4\sqrt{r}$ , and  $\epsilon \in (0, \frac{1}{2})$ , we say a city has  $(\beta, \epsilon)$ -**urbanized segregation** if it is both  $(\beta, \epsilon)$ -segregated and has  $\epsilon$ -urbanization of poverty.*

Like Definition 5,  $\beta$  here controls how small the boundary is between the red region  $R$  and the rest of the city, while  $\epsilon$  expresses the tolerance for having agents of the wrong color within the monochromatic color regions or having rich agents on the urban sites. In the

following theorem, we show that for large enough  $\lambda$  and  $\gamma$ , with high probability,  $\mathcal{M}$  leads to urbanized segregation. See Figure 3a for simulated visualizations.

**Theorem 7 (Urbanized Racial Segregation).** *With centralized urban sites,  $\lambda > 3^{\frac{\alpha}{\beta}} 4^{\frac{3\delta+1}{4\delta}}$ ,  $\gamma^{\delta/3} > 4^{\frac{3\delta+1}{4\delta}}$ , and  $n$  sufficiently large, configurations from  $\mathcal{M}$  drawn from distribution  $\pi$  have  $(\beta, \epsilon)$ -urbanized segregation with probability at least  $1 - \xi\sqrt{n}$  for some constant  $0 < \xi < 1$ , and  $\delta = \frac{\epsilon}{2}$ .*

**PROOF OF THEOREM 7.** First, we define  $U_{\beta, \epsilon} \subset \Omega$  to be the configurations that have  $(\beta, \epsilon)$ -urbanized segregation. To prove Theorem 7, it suffices to prove  $\pi(\Omega \setminus U_{\beta, \epsilon}) \leq \xi\sqrt{n}$ , where  $\xi \in (0, 1)$ . We can further divide  $\Omega \setminus U_{\beta, \epsilon}$  into two parts:  $\Omega_{\text{-urb}}$  that do not have  $\epsilon$ -urbanization of poverty, and  $\Omega_{\text{urb}\wedge\text{-seg}}$  that have  $\epsilon$ -urbanization of poverty and do not have  $(\beta, \epsilon)$ -segregation. Thus it suffices to prove  $\pi(\Omega_{\text{-urb}}) \leq \xi_1^n$  and  $\pi(\Omega_{\text{urb}\wedge\text{-seg}}) \leq \xi_0\sqrt{n}$ , for  $0 < \xi_1, \xi_0 < 1$ . It follows from the proof of Theorem 2 that if  $\lambda \geq 4^{\frac{3\delta+1}{4\delta}}$ , as long as  $\gamma^{\delta/3} > 4^{\frac{3\delta+1}{4\delta}}$ ,  $\pi(\Omega_{\text{-urb}}) \leq \xi_1^n$ . It is proved in Claim 20 in Section 5 of SI that if  $\lambda > 3^{\frac{\alpha}{\beta}} 4^{\frac{3\delta+1}{4\delta}}$ ,  $\pi(\Omega_{\text{urb}\wedge\text{-seg}}) \leq \xi_0\sqrt{n}$  for some  $\xi_0 \in (0, 1)$ . Combining the two parts, to have  $\pi(\Omega \setminus U_{\beta, \epsilon})$  to be exponentially small for large  $n$ , it suffices to have  $\lambda > 3^{\frac{\alpha}{\beta}} 4^{\frac{3\delta+1}{4\delta}}$  and  $\gamma^{\delta/3} > 4^{\frac{3\delta+1}{4\delta}}$ .  $\square$

To complement Theorem 7, we prove that for large enough  $\gamma$  but  $\lambda > 1$  below a threshold, we will likely observe urbanization of poverty but racial integration outside the urban area under certain demographic parameter choices. The proof technique is very similar to the proof of Theorem 4. See Section 6 of SI for proof details. A special case of Theorem 8 is shown in Remark 9, where segregation of poor red agents occurs inside the urban area and racial integration occurs outside. See Figure 3b for simulated visualizations.

**Theorem 8 (Coexistence of Urbanization and Racial Integration).** *With the centralized urban sites, for the demographics choices such that  $(\frac{p-\delta}{r_p})r_p(\frac{1-p-\delta}{r_r})r_r > 2^r$ , if  $1 < \lambda^3 < (\frac{p-\delta}{b_p})b_p(\frac{1-p-\delta}{b_r})b_r/2^r$ , and  $\gamma^{\delta/3} > 16^{\frac{3\delta+1}{4\delta}}$ , when  $n$  is sufficiently large, then for  $\mathcal{M}$ , configurations drawn from distribution  $\pi$  have  $\epsilon$ -urbanization of poverty and are integrated outside the urban area with probability at least  $1 - \xi_3^n$  for some constant  $0 < \xi_3 < 1$  and  $\delta = \frac{\epsilon}{2}$ .*

**Remark 9.** *As a special case when the size of the urban sites can roughly accommodate all of poor agents, where  $p < c < p + \epsilon$ , if the demographics satisfies Theorem 8 with  $b_p \leq m\epsilon$ , then under the same bias parameter choices as Theorem 8, then with high probability the stationary configuration will have urbanized segregation of poor red agents, where the density of poor red on the urban sites is at least  $1 - (m+1)\epsilon$ , and racial integration of the rich outside the urban area.*

**PROOF OF THEOREM 8.** We define  $\Omega_{\text{urb}\wedge\text{-seg}} \subset \Omega$  to be the configurations that have  $\epsilon$ -urbanization of the poor and  $(\beta, \delta)$ -integration outside the urban area. It suffices to show that with all but exponentially small probability, a sample drawn from (3) is not in  $\Omega_{\text{urb}\wedge\text{-seg}}$ :  $\pi(\Omega \setminus \Omega_{\text{urb}\wedge\text{-seg}}) \leq \xi_3\sqrt{n}$ , where  $\xi_3 \in (0, 1)$  and  $n$  is sufficiently large.

We can further divide the configuration space  $\Omega \setminus \Omega_{\text{urb}\wedge\text{-seg}}$  into two parts: the set of configurations  $\Omega_{\text{-urb}}$  that do not have  $\epsilon$ -urbanization of poverty, and the set of configurations  $\Omega_{\text{urb}\wedge\text{seg}}$  that have  $\epsilon$ -urbanization of poverty and  $(\beta, \delta)$ -segregation. Since  $\Omega \setminus \Omega_{\text{urb}\wedge\text{-seg}} = \Omega_{\text{-urb}} + \Omega_{\text{urb}\wedge\text{seg}}$ , to prove  $\pi(\Omega \setminus \Omega_{\text{urb}\wedge\text{-seg}}) \leq \xi_3\sqrt{n}$ , it suffices to prove  $\pi(\Omega_{\text{-urb}}) \leq \xi_1^n$  and  $\pi(\Omega_{\text{urb}\wedge\text{seg}}) \leq \xi_0\sqrt{n}$ , for some constant  $0 < \xi_1, \xi_0 < 1$  and sufficiently large  $n$ .

It follows from Theorem 2 that for  $\gamma^{\delta/3} > 16^{\frac{3\delta+1}{4\delta}}$  and  $\lambda > 1$ ,  $\pi(\Omega_{\text{-urb}}) \leq \xi_1^n$  for some  $\xi_1 \in (0, 1)$ . To prove the second part  $\pi(\Omega_{\text{urb}\wedge\text{seg}}) \leq \xi_0\sqrt{n}$ , for each  $\sigma \in \Omega_{\text{urb}\wedge\text{seg}}$ , we construct a  $\delta$ -color bridge system (see Section 1.2 of SI for definition). Then we define the mapping  $s = (s_2 \circ f_2)(\cdot)$ : we do the color inversion and obtain  $\tau = f_2(\sigma)$ ; next for  $\tau$ , we randomly flip the cyan to pink until the right number of the pink, and we randomly flip the blue to red until the right number of the red and obtain  $\nu = s_2(\tau)$ .

Finally, we define a weighted bipartite graph  $G(\Omega_{\text{urb}\wedge\text{seg}}, \Omega, E)$  with an edge of weight  $\pi(\sigma)$  between  $\sigma \in \Omega_{\text{urb}\wedge\text{seg}}$  and  $\nu \in \Omega$ . The total weight of edges is

$$\begin{aligned} & \sum_{\sigma \in \Omega_{\text{urb}\wedge\text{seg}}} \pi(\sigma) \cdot |S(\sigma)| \\ & \geq \pi(\Omega_{\text{urb}\wedge\text{seg}}) \left( \frac{p-\delta}{r_p} \right)^{(r_p-\delta)n} \left( \frac{1-p-\delta}{r_r} \right)^{(r_r-\delta)n}. \end{aligned} \quad (4)$$

On the other hand, the weight of the edges is at most

$$\begin{aligned} & \sum_{\nu \in \Omega} \sum_{\sigma \in s^{-1}(\nu)} \max_{\sigma \in \Omega_{\text{urb}\wedge\text{seg}}} \pi(\sigma) \\ & = \sum_{\nu \in \Omega} \pi(\nu) \sum_{\sigma \in s^{-1}(\nu)} \frac{\max_{\sigma \in \Omega_{\text{urb}\wedge\text{seg}}} \pi(\sigma)}{\pi(\nu)} |s^{-1}(\nu)| \\ & \leq \sum_{\nu \in \Omega} \pi(\nu) \sum_{z_c = \sqrt{m}}^{\beta\sqrt{n}} l \cdot \lambda^{\max(h(\nu)-h(\sigma))} \gamma^{\max(p(\sigma)-p(\nu))} 4^{\frac{3\delta+1}{4\delta} z_c} 2^{rn} \\ & \leq \sum_{z_c = \beta_{\min}\sqrt{n}}^{\beta\sqrt{n}} l \cdot \left( \frac{4^{\frac{3\delta+1}{4\delta}}}{\lambda} \right)^{z_c} \lambda^{3n} 2^{rn}. \end{aligned} \quad (5)$$

where  $l \triangleq (z_c + 1)3^{\alpha\sqrt{n}}$ , and the inequalities in Claims 23-25 from Section 6 of SI have been substituted in the above derivation. Combining equations (4) and (5), we find

$$\begin{aligned} & \pi(\Omega_{\text{urb}\wedge\text{seg}}) \left( \frac{p-\delta}{r_p} \right)^{(r_p-\delta)n} \left( \frac{1-p-\delta}{r_r} \right)^{(r_r-\delta)n} \\ & \leq \sum_{z_c = \beta_{\min}\sqrt{n}}^{\beta\sqrt{n}} (z_c + 1)3^{\alpha\sqrt{n}} \left( \frac{4^{\frac{3\delta+1}{4\delta}}}{\lambda} \right)^{z_c} \lambda^{3n} 2^{rn}. \end{aligned} \quad (6)$$

For large enough  $n$ , to have  $\pi(\Omega_{\text{urb}\wedge\text{seg}}) \leq \xi_3^n$  for some  $\xi_3 \in (0, 1)$ , it suffices to have

$$\begin{aligned} \lambda^{3n} 2^{rn} & < \left( \frac{p-\delta}{r_p} \right)^{(r_p-\delta)n} \left( \frac{1-p-\delta}{r_r} \right)^{(r_r-\delta)n} \\ & < \left( \frac{p-\delta}{r_p} \right)^{r_p n} \left( \frac{1-p-\delta}{r_r} \right)^{r_r n}, \end{aligned}$$

which can be rewritten as

$$\lambda^3 < \left( \frac{p-\delta}{r_p} \right)^{r_p} \left( \frac{1-p-\delta}{r_r} \right)^{r_r} / 2^r.$$

Since  $\lambda > 1$ , to make the right hand side of the above inequality greater than one, it suffices to have  $(\frac{p-\delta}{r_p})r_p(\frac{1-p-\delta}{r_r})r_r > 2^r$ . Combining the above parameter choices with Theorem 2 requires  $\gamma^{\delta/3} > 16^{\frac{3\delta+1}{4\delta}}$  and  $\lambda > 1$ , proving Theorem 8.  $\square$

## 6 INTEGRATION IN CITIES WITH DISTRIBUTED URBAN SITES

As we've shown, when urban sites are centralized, the wealth and homophily biases align to cause segregation, as shown in Theorem 7. However, when the placement of urban sites is *distributed*, the racial and wealth biases will work against each other, and we will get integration if the influence of the wealth bias exceeds the homophily bias. See Figure 3b for simulations.

**Theorem 10.** *In a city with  $|\mathcal{U}| = cn$  urban sites evenly partitioning in the city (like we find with bus routes), a small number of poor blue agents, with  $b_p < \hat{b}_p$ , and any  $\lambda > 1$ , if  $\gamma^{\hat{b}_p - b_p} > \lambda^{2c} 64^{\frac{3\delta+1}{4\delta}}$ , and  $n$  sufficiently large, then configurations drawn from distribution  $\pi$  will be  $(\beta, \delta)$ -segregated with exponentially small probability  $\xi_4^n$ , for some constant  $0 < \xi_4 < 1$ .*

Hence, integration occurs because no matter how large the homophily bias weight  $\lambda^{-(h(\sigma)-h(v))}$  is, as long as the energy term arising from the wealth bias  $\gamma^{p(\sigma)-p(v)}$  is larger, then the stationary distribution will be very unlikely to be segregated. See below for the proof.

**PROOF OF THEOREM 10.** We define the configuration space  $S_{\beta,\delta}$  to be the set of configurations that are  $(\beta, \delta)$ -segregated. To prove Theorem 10, it suffices to prove  $\pi(S_{\beta,\delta}) \leq \xi_4^n$ , where  $\xi_4 \in (0, 1)$ . The bridging and the mapping  $\nu = f(\sigma) = (f_5 \circ f_4 \circ f_3 \circ f_2 \circ f_1)(\sigma)$  are defined as the following: we first construct a  $\delta$ -race\_wealth bridge system for  $\sigma \in S_{\beta,\delta}$  (see Section 1.2 of SI for details). Then we do richness inversion and color inversion like defined in  $f_1(\cdot)$  and  $f_2(\cdot)$ . Then we do the color and richness recovery  $\nu = (f_5 \circ f_4 \circ f_3 \circ f_2)(\tau)$  in the distributed way as specified in Section 1.5 of SI. After the mapping, it is proved in Claim 26 of SI that for any  $\sigma \in S_{\beta,\delta}$  with a given bridged color contour length  $z_c$ ,  $h(\nu) - h(\sigma) \leq 2cn - z_c$  and  $p(\sigma) - p(\nu) \leq b_p n - \hat{b}_p n$ , where  $\hat{b}_p \triangleq \min\{c, p\} - (r + \delta)c - 2\delta$ . See proof details of Claim 26 from Section 7 of SI.

For a given color contour length  $z_c$ , for any  $\nu = f(\sigma)$ , the number of preimages follows from Claim 16. Similarly, we use Peierls argument (1), substituting the related bounds into which yields

$$\pi(S_{\beta,\delta}) \leq \sum_{\nu \in \Omega} \pi(\nu) \sum_{z_c = \sqrt{r \cdot n}}^{\beta \sqrt{n}} n^6 (3n + 1) (z_c + 1) 9^{\alpha \sqrt{n}} \left( \frac{4^{\frac{3\delta+1}{4\delta}}}{\lambda} \right)^{z_c} \left( \frac{\lambda^{2c} 64^{\frac{3\delta+1}{4\delta}}}{\gamma^{\hat{b}_p - b_p}} \right)^n,$$

where  $z_c \geq \sqrt{r \cdot n}$  is due to the triangular lattice geometry, which is proved in Lemma 2.1 in [6], and  $z_c \leq \beta \sqrt{n}$  is due to  $\sigma \in S_{\beta,\delta}$  and the definition of  $(\beta, \delta)$ -segregation. If  $b_p < \hat{b}_p$  and  $\gamma^{\hat{b}_p - b_p} > \lambda^{2c} 64^{\frac{3\delta+1}{4\delta}}$ , the sum will be exponentially small given large enough  $n$ , which means  $\pi(S_{\beta,\delta}) \leq \xi_4^n$  for some  $\xi_4 \in (0, 1)$ .  $\square$

**Remark 11.** *If the number of poor blue agents satisfies  $b_p < \hat{b}_p \triangleq \min\{c, p\} - (r + \delta)c - 2\delta$ , we can conclude the ratio between poor*

*blue and poor red agents is smaller than the ratio between the blue and the red:  $\frac{b_p}{r_p} < \frac{b_r}{r_r}$ , which is understood as income inequality.*

**PROOF.** If  $c \leq p$ , then it follows that  $b_p < c - (r + \delta)c - 2\delta = (b - \delta)c - 2\delta < (b - \delta)c < (b - \delta)p < b \cdot p$ , which can be written as  $\frac{b_p}{r_p} < \frac{b \cdot p}{r_p} = b + b \cdot \frac{b_p}{r_p}$ . Hence we can get  $\frac{b_p}{r_p} < \frac{b}{r}$ . If  $p \leq c$ , it follows that  $b_p < p - (r + \delta)c - 2\delta < p - (r + \delta)p - 2\delta < p(b - \delta) < b \cdot p$ . Hence the same conclusion  $\frac{b_p}{r_p} < \frac{b}{r}$  follows.  $\square$

**Remark 12.** *Although Theorem 10 is proved under the lattice-shaped urban sites shown in Figure 1b. But urban sites can also be distributed in other ways and a similar proof will follow, like many (order of  $O(n)$ ) small clusters of disconnected urban sites.*

## 7 SIMULATIONS

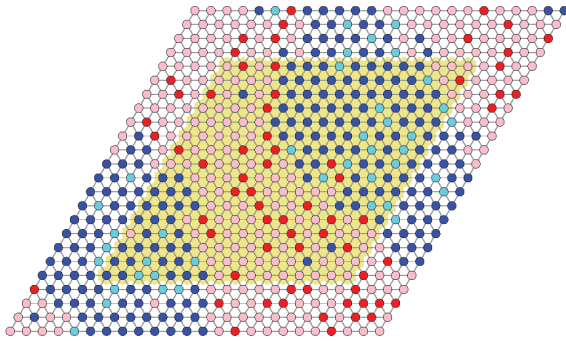
We supplement the theorems with simulations of  $\mathcal{M}$ , shown in Figure 2, 3, and 4, for a city with income inequality starting from random initial locations of agents. Figure 2 compares configurations after running  $\mathcal{M}$  for the same number of iterations, varying only the values of  $\lambda$ ,  $\gamma$ , and the placement of urban sites. Note that the parameter settings for  $\lambda$  and  $\gamma$  in the simulations are better than in our theorems, confirming that our bounds are likely not tight.

Figure 2a demonstrates Theorems 2 and 8 showing the coexistence of urbanization of poverty and racial integration outside the urban area under strong wealth bias but slight racial bias. Specially, since the chosen urban area can accommodate all the poor agents in a city and the city has severe income inequality, Figure 2a can also be viewed as a verification of Remark 9, showing segregation of poor red agents in the urban area and integration outside. Individuals in Figure 2a have small racial biases, so the wealth biases can also drive racial segregation under the centralized placement of urban sites. Figure 2b verifies Corollary 3, showing the urbanization of poverty with distributed urban sites. Compared with Figure 2a, the pink cluster gets dispersed via the distributed urban sites. Figure 3a verifies Theorem 7, showing the urbanized segregation. Due to income inequality, where most of the poor agents are red, we can see that the pink predominantly occupies the urban area. In contrast, in Figure 5, when there is income equality across races, we can see urbanized segregation and roughly the same amount of poor red and poor blue agents occupying the urban sites. Figure 3b demonstrates Theorem 10, showing the mitigation of segregation via distributing the urban sites in the existence of agents' strong racial bias, which should lead to Figure 3a urban sites are not distributed. Compared with Figure 2b, whose segregation level is even smaller, the difference is that agents in Figure 2b have little racial bias, whereas in Figure 3b each agent has strong racial bias. Figures 4a and 4b provide baselines of the main work. Figure 4a shows segregation under strong racial bias without wealth bias, which was proved in [5, 21]. Figure 4b shows integration under little racial and wealth bias, which is proved in Theorem 4.

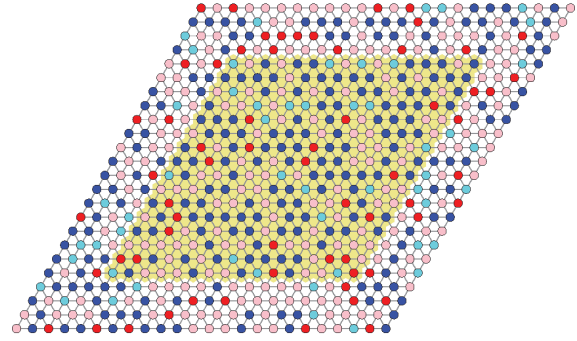
## 8 CONCLUSIONS

In this work, we consider the interplay of race and socioeconomic status by introducing a heterogeneous stochastic Schelling model with urban sites as incentives for the poor individuals. We show





(a) segregation no wealth bias when  $\gamma = 1, \lambda = 2$ .



(b) integration with  $\gamma = 1.01, \lambda = 1.01$ .

**Figure 4: Simulations of  $\mathcal{M}$  after five million iterations with 40% poor red(pink), 10% rich red (red), 40% rich blue (blue), and 10% poor blue (cyan) and a 46% fraction of the urban sites.**

that compact and centralized urban sites, like in a city center, encourage poor agents to cluster centrally, while infrastructure that is well distributed, like a large grid of bus routes spanning the entire city, tends to disperse the low-income agents. Understanding the effects of these two scenarios on segregation can be helpful for understanding how to best distribute public amenities to help mitigate segregation.

We find that centralized infrastructure simultaneously causes an “urbanization of poverty” (i.e., occupation of urban sites primarily by poor agents) and segregation when both the homophily and incentives drawing poor agents to urban sites are large enough. Moreover, if there is *income inequality* where one race has a significantly higher proportion of poor agents, when homophily preferences are small and incentives drawing the poor individuals to urban sites are sufficiently large, we get racial *segregation* on urban sites and *integration* on non-urban sites, with high probability. However, we find there is overall mitigation of segregation (on urban and non-urban sites) whenever the urban sites are spatially distributed

throughout the lattice and the incentives drawing poor agents to the urban sites exceed the homophily preference. We prove that in this case, no matter how strong homophily preferences are, it will be exponentially unlikely that a configuration chosen from stationarity will have large, homogeneous clusters of similarly colored agents, thus promoting integration in the city. These findings suggest that deliberate urban planning can mitigate or enhance segregation.

We note that there are many limitations of the heterogeneous Schelling model studied here, with many variants worth considering. For instance, in addition to amenities that are only preferred by poor agents, we can introduce other amenities preferred by rich agents [19], such as fine arts and various recreational services. We intend to introduce such incentives for the rich in subsequent work.

Naturally, the model considered here is an abstraction that oversimplifies biases and ignores many factors affecting segregation and incentives in the real world. Many other important factors, such as housing prices and individuals’ preferences for higher-income neighbors, are not captured in our model. Nonetheless, we believe that this simple model can provide insight into how socioeconomic incentives might worsen or mitigate segregation through the allocation of urban amenities. To supplement the theoretical findings presented here, we also are exploring relevant demographic data in cities across the United States [34]. After collecting national data, we find some positive correlations between cities with more distributed amenities and better racial integration, as found in our model.

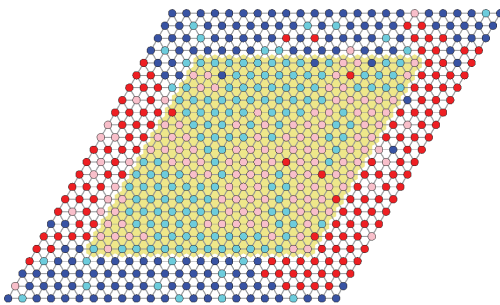


**Figure 5: Urbanized segregation without income inequality under strong wealth and racial biases ( $\gamma = 200, \lambda = 1.01$ ). The racial and wealth distribution is 25% poor red, 25% rich red, 25% rich blue, and 25% poor blue.**

## REFERENCES

- [1] George Barmpalias, Richard Elwes, and Andy Lewis-Pye. 2014. Digital morphogenesis via Schelling segregation. In *2014 IEEE 55th Annual Symposium on Foundations of Computer Science*. IEEE, 156–165.
- [2] Patrick Bayer and Robert McMillan. 2012. Tiebout sorting and neighborhood stratification. *Journal of Public Economics* 96, 11–12 (2012), 1129–1143.
- [3] Prateek Bhakta, Sarah Miracle, and Dana Randall. 2014. Clustering and Mixing Times for Segregation Models on  $\mathbb{Z}^2$ . In *Proceedings of the twenty-fifth annual ACM-SIAM symposium on Discrete algorithms*. SIAM, 327–340.
- [4] Christina Brandt, Nicole Immerlica, Gautam Kamath, and Robert Kleinberg. 2012. An analysis of one-dimensional Schelling segregation. In *Proceedings of the forty-fourth annual ACM symposium on Theory of computing*. 789–804.

- [5] Sarah Cannon, Joshua J. Daymude, Cem Gokmen, Dana Randall, and Andréa W. Richa. 2019. A local stochastic algorithm for separation in heterogeneous self-organizing particle systems. *Proceedings of RANDOM* (2019).
- [6] Sarah Cannon, Joshua J. Daymude, Dana Randall, and Andréa W. Richa. 2016. A Markov chain algorithm for compression in self-organizing particle systems. In *Proceedings of the 2016 ACM Symposium on Principles of Distributed Computing*. 279–288.
- [7] William A.V. Clark. 1991. Residential preferences and neighborhood racial segregation: A test of the Schelling segregation model. *Demography* 28, 1 (1991), 1–19.
- [8] William A.V. Clark and Mark Fossett. 2008. Understanding the social context of the Schelling segregation model. *Proceedings of the National Academy of Sciences* 105, 11 (2008), 4109–4114.
- [9] Marie Cottrell, Madalina Olteanu, Julien Randon-Furling, and Aurelien Hazan. 2017. Multidimensional urban segregation: an exploratory case study. In *2017 12th International Workshop on Self-Organizing Maps and Learning Vector Quantization, Clustering and Data Visualization (WSOM)*. IEEE, 1–7.
- [10] William Feller. [n.d.]. An introduction to probability theory and its applications. 1957 ([n. d.]).
- [11] Mark Fossett. 2011. Generative models of segregation: Investigating model-generated patterns of residential segregation by ethnicity and socioeconomic status. *The Journal of mathematical sociology* 35, 1-3 (2011), 114–145.
- [12] Stefan Gerhold, Lev Glebsky, Carsten Schneider, Howard Weiss, and Burkhard Zimmermann. 2008. Computing the complexity for Schelling segregation models. *Communications in Nonlinear Science and Numerical Simulation* 13, 10 (2008), 2236–2245.
- [13] Edward L. Glaeser, Matthew E. Kahn, and Jordan Rappaport. 2008. Why do the poor live in cities? The role of public transportation. *Journal of urban Economics* 63, 1 (2008), 1–24.
- [14] Erez Hatna and Itzhak Benenson. 2014. Combining segregation and integration: Schelling model dynamics for heterogeneous population. *arXiv preprint arXiv:1406.5215* (2014).
- [15] John Iceland, Daniel H. Weinberg, and Erika Steinmetz. 2002. *Racial and ethnic residential segregation in the United States 1980-2000*. Vol. 8. Bureau of Census.
- [16] Katherine Kortum, Rajesh Paleti, Chandra R. Bhat, and Ram M. Pendyala. 2012. Joint model of residential relocation choice and underlying causal factors. *Transportation research record* 2303, 1 (2012), 28–37.
- [17] Alexander J. Laurie and Narendra K. Jaggi. 2003. Role of 'vision' in neighbourhood racial segregation: a variant of the Schelling segregation model. *Urban Studies* 40, 13 (2003), 2687–2704.
- [18] Sonia Lehman-Frisch. 2011. Segregation, spatial (in) justice, and the city. *Berkeley Planning Journal* 24, 1 (2011).
- [19] Stephen F LeRoy and Jon Sonstelie. 1983. Paradise lost and regained: Transportation innovation, income, and residential location. *Journal of urban economics* 13, 1 (1983), 67–89.
- [20] David A. Levin and Yuval Peres. 2017. *Markov chains and mixing times*. Vol. 107. American Mathematical Soc.
- [21] Shengkai Li, Bahnisikha Dutta, Sarah Cannon, Joshua J. Daymude, Ram Avinery, Enes Aydin, Andréa W. Richa, Daniel I. Goldman, and Dana Randall. 2021. Programming active cohesive granular matter with mechanically induced phase changes. *Science Advances* 7, 17 (2021), eabe8494.
- [22] Douglas S. Massey and Nancy A. Denton. 1988. The dimensions of residential segregation. *Social forces* 67, 2 (1988), 281–315.
- [23] Sarah Miracle, Dana Randall, and Amanda Pascoe Streib. 2011. Clustering in interfering binary mixtures. In *Approximation, Randomization, and Combinatorial Optimization. Algorithms and Techniques*. Springer, 652–663.
- [24] Rocco Paolillo and Jan Lorenz. 2018. How different homophily preferences mitigate and spur ethnic and value segregation: Schelling's model extended. *Advances in Complex Systems* 21, 06n07 (2018), 1850026.
- [25] Liliana Perez, Suzana Dragicevic, and Jonathan Gaudreau. 2019. A geospatial agent-based model of the spatial urban dynamics of immigrant population: A study of the island of Montreal, Canada. *Plos one* 14, 7 (2019), e0219188.
- [26] Mark Pollicott and Howard Weiss. 2001. The dynamics of Schelling-type segregation models and a nonlinear graph Laplacian variational problem. *Advances in Applied Mathematics* 27, 1 (2001), 17–40.
- [27] Anand Sahasranaman and Henrik Jeldtoft Jensen. 2018. Ethnicity and wealth: The dynamics of dual segregation. *PloS one* 13, 10 (2018), e0204307.
- [28] Thomas C. Schelling. 1971. Dynamic models of segregation. *Journal of mathematical sociology* 1, 2 (1971), 143–186.
- [29] Abhinav Singh, Dmitri Vainchtein, and Howard Weiss. 2009. Schelling's segregation model: Parameters, scaling, and aggregation. *Demographic Research* 21 (2009), 341–366.
- [30] Dietrich Stauffer. 2008. Social applications of two-dimensional Ising models. *American Journal of Physics* 76, 4 (2008), 470–473.
- [31] Dietrich Stauffer and Sorin Solomon. 2007. Ising, Schelling and self-organising segregation. *The European Physical Journal B* 57, 4 (2007), 473–479.
- [32] Tiit Tammaru, Szymon Marcińczak, Raivo Aunap, Maarten van Ham, and Heleen Janssen. 2020. Relationship between income inequality and residential segregation of socioeconomic groups. *Regional Studies* 54, 4 (2020), 450–461.
- [33] John Yinger. 1976. Racial prejudice and racial residential segregation in an urban model. *Journal of urban economics* 3, 4 (1976), 383–396.
- [34] Zhanzhan Zhao, Chisun Yoo, Nima Golshani, Catherine Ross, and Dana Randall. 2022. National and Regional Correlations between Public Amenities and Racial Segregation in U.S. Cities. *in preparation* (2022).